International Journal of Environmental Sciences
ISSN: 2229-7359
Vol. 11 No. 7s, 2025
https://www.theaspd.com/ijes.php

Formulation And Characterization Of Silver Nanoparticles Incorporated Gel Of Ethanolic Extract Of Celastrus Orbiculatus For Effective Antimicrobial Effect

Richa Tripathi*, Vivek Chourasia

Mansarovar Global University, Bhopal (M.P.)
Corresponding author mail id: richatrpth527@gmail.com

Abstract

The present study focuses on the green synthesis of silver nanoparticles (AgNPs) using the ethanolic extract of Celastrus orbiculatus and their incorporation into hydrogel formulations for enhanced topical antimicrobial activity. Various nanoparticle formulations (F1–F9) were evaluated for percentage yield, entrapment efficiency, and particle size, with formulation F2 identified as the optimized batch. Characterization using FTIR, UV–Vis spectroscopy, and SEM confirmed successful nanoparticle synthesis and morphology. The optimized AgNPs were incorporated into hydrogel formulations (G1–G6), with G3 selected as the optimal gel based on its physicochemical properties, including high drug content (4.05 ± 0.25 mg/100 mg), appropriate pH, viscosity, spreadability, and extrudability. In-vitro drug release from G3 followed a diffusion-controlled mechanism (Higuchi model, $r^2 = 0.9779$). Antimicrobial studies revealed that the AgNP-loaded gel (G3) showed significantly greater zones of inhibition against Staphylococcus aureus and Klebsiella pneumoniae compared to the crude extract. These results highlight the potential of green-synthesized AgNP hydrogels as effective topical antimicrobial agents.

Keywords: *Celastrus orbiculatus, silver nanoparticles, hydrogel, green synthesis, antimicrobial activity, in-vitro drug release, topical formulation, entrapment efficiency, FTIR, SEM.*

INTRODUCTION

Nanotechnology has emerged as a revolutionary platform in biomedical research, offering innovative solutions in drug delivery, diagnostics, and antimicrobial therapy. Among various nanomaterials, silver nanoparticles (AgNPs) have garnered significant attention due to their broad-spectrum antimicrobial properties, biocompatibility, and ability to overcome antibiotic resistance mechanisms in pathogenic microorganisms (Rai et al., 2009). The biological synthesis of AgNPs using plant extracts, commonly referred to as green synthesis, offers a safer, eco-friendly, and cost-effective alternative to conventional chemical and physical methods (Iravani et al., 2014). Phytochemicals such as flavonoids, phenols, and alkaloids present in plant extracts play a crucial role in reducing silver ions and stabilizing the synthesized nanoparticles.

Celastrus orbiculatus, a medicinal plant widely used in traditional medicine, is known for its diverse pharmacological properties including anti-inflammatory, antioxidant, and antimicrobial activities (Xiao et al., 2015). Previous phytochemical studies have confirmed the presence of bioactive constituents such as flavonoids, alkaloids, and phenolic compounds in its ethanolic extract, which not only impart therapeutic efficacy but also contribute to the reduction and capping processes during nanoparticle synthesis. The synergistic integration of AgNPs with plant-based bioactives may enhance antimicrobial potency, making it a promising strategy for topical applications.

Formulating AgNPs into a topical gel base ensures controlled drug release, localized action, and improved patient compliance (Kora & Arunachalam, 2011). The incorporation of AgNPs synthesized from the ethanolic extract of Celastrus orbiculatus into a gel matrix may offer a potent antimicrobial system suitable for treating skin infections and wounds. This study aims to formulate and characterize a silver nanoparticle-

loaded gel containing the ethanolic extract of Celastrus orbiculatus and evaluate its antimicrobial potential against common pathogenic bacteria.

MATERIAL AND METHODS

Material

The investigation utilized fresh, shade-dried leaves of Celastrus orbiculatus collected locally and authenticated for ethanolic extraction. Silver nitrate ($AgNO_3$, ≥99% purity) was obtained from Sigma-Aldrich, India, and absolute ethanol (99.9%) was sourced from Merck India Ltd., Mumbai. Carbopol 934 (used as a gelling agent) was procured from Sulab, India. Triethanolamine (used for gel neutralization) and glycerin (humectant) were supplied by Loba Chemie Pvt. Ltd., Mumbai. Double distilled water was prepared in-house. All chemicals used were of analytical or reagent grade, suitable for biological and pharmaceutical applications.

METHODS

Collection of Celastrus orbiculatus

The Minor Forest Produce Processing & Research Centre, Vindhya Herbals Bhopal, is where Celastrus orbiculatus leaves were gathered. Normal tap water was used to completely wash the plant materials, and then sterile distillation water was used. Then allowed to air dry at ambient temperature in a shady area. A grinding machine was used to crush the dried plant materials into a powder. The powder was kept in a bottle with a tight air container at 4°C.

Extraction by maceration method

Through a maceration procedure, 80 grams of powdered Celastrus orbiculatus leaves were thoroughly extracted using a variety of solvents, including ethanol. Below their boiling temperatures, the extracts were evaporated. Lastly, the dried extracts yield % was calculated. After being recovered, the extracts were reduced in a rotary evaporator and then kept for later use in airtight containers at 4°C.

Synthesis of Silver nanoparticles of ethanolic extract of Celastrus orbiculatus

50 ml of double distilled water was added to a wide neck borosil flask containing roughly 250 mg of Celastrus orbiculatus leaf extract (semi-solid mass). This flask was heated in a microwave for 3 minutes in order to weaken the proteins and enzymes that obstruct the reduction process. The manufacture of nanoparticles was carried out using the clear filtrate that was produced by the aforementioned process. 50 ml of various quantities of silver nitrate solution (0.1 M, 0.01 M, and 0.001 M) were mixed with this extract in the following ratios: 1:1, 1:1, and 1:1, respectively, and then exposed to microwave radiation. A pale yellowish hue was seen as soon as the plant extract solution was added to the AgNO3 aqueous solution. This color turned to a dark brown when exposed to microwave radiation, and it intensified with subsequent exposure.

The occurrence of this color shift signifies the creation of AgNPs. Centrifugation was used to separate the mixtures different components. Following centrifugation of the aforementioned solution at 4000 rpm for 20 minutes, the supernatant was centrifuged again at 20000 rpm for 30 minutes. After giving the resulting residue a thorough wash with double-distilled water, 100 ml of the water were added. To determine the weight of the isolated AgNPs (together with the Celastrus orbiculatus component), the solution was vacuum dried (Raghunandan et al., 2021).

Table 1: Formulation optimization of silver nanoparticles of Celastrus orbiculatus extract

F. Code	Ethanolic Extract	$AgNO_3$ (M)	Ratio
F1	250	0.1	1:1
F2	250	0.1	1:1
F3	250	0.1	1:1
F4	250	0.01	1:1
F5	250	0.01	1:1
F6	250	0.01	1:1
F7	250	0.001	1:1
F8	250	0.001	1:1
F9	250	0.001	1:1

Characterization of silver nanoparticles

To comprehend the physical, chemical, and biological characteristics of silver nanoparticles (AgNPs), characterisation is an essential first step. To verify the effective synthesis and ascertain the nanoparticles size, shape, surface morphology, and crystalline nature, a variety of analytical techniques are used.

The surface plasmon resonance (SPR) of silver nanoparticles, which is routinely detected in the 400–450 nm range and offers initial evidence of nanoparticle synthesis, is frequently monitored using UV-visible spectroscopy. The functional groups in the plant extract or reducing agents that are in charge of lowering the silver ions and stabilizing the nanoparticles can be found using Fourier Transform Infrared Spectroscopy (FTIR). SEM, or scanning electron microscopy, offers comprehensive details on the size, shape, and morphology of particles. Furthermore, the hydrodynamic diameter and size distribution are ascertained by Dynamic Light Scattering, and the surface charge and colloidal stability of the nanoparticles are assessed by Zeta potential analysis.

Percentage yield

The weight of the final AgNPs was divided by the total quantity of non-volatile ingredients that went into making them (Bahuguna et al., 2016).

$$\% \text{ Yield } = \frac{\text{Actual weight of product}}{\text{Total weight of drug and polymer}} \text{x } 100$$

Entrapment efficiency

Using an Eppendorf centrifuge, 1.5 ml of the formulation was precisely centrifuged for 45 minutes at 4°C at 13,000 rpm (Bar et al., 2009). Using a micropipette, the supernatant was extracted, and its flavonoid concentration was determined using the UV technique. The following formula was used to determine the percentage of drug encapsulation:

EE (%) = (Ct - Cr) / Ct × 100

where Cr is the amount of free drug in the supernatant and Ct is the amount of drug added.

Surface charge and particle size

The size, distribution, and electric charge of the particles were determined using the Dynamic Light Scattering (DLS) technique (SAIF RGPV Bhopal, Malvern Zetamaster, ZEM 5002, Malvern, UK) (Guzman et al., 2009). To measure and ascertain the zeta potential, a measuring cell with a large diameter was subjected to a zeta sizer with a field strength of 20 V/cm. The samples were diluted with a 0.9% NaCl solution to reach a conductivity of 50 lS/cm4.

FT-IR Analysis of silver nanoparticles

Using a Fourier Transform Infrared Spectrophotometer and the KBr method, the extracts and the generated silver nanoparticles IR spectra were acquired (Ibrahim, 2015). A dried potassium bromide pellet was used to make a baseline correction. The components were ground and compressed in a pressure compression machine to create a pellet with a diameter of roughly 1 mm. It contained a physical combination of 5 mg of extract and AgNPs separately, together with 100–150 mg of potassium bromide. After being put in the infrared compartment, the supplied pellet was scanned between wavelengths ranging from 4000 cm-1 to 400 cm-1.

Ultraviolet-Visible Spectral Analysis

A UV-visible spectrometer (Labindia 3000+) was used to measure the UV-absorption spectra of the generated AgNPs. The spectra were scanned between 200-400 nm (Kumar et al., 2011).

Scanning electron microscopy (SEM)

Using a scanning electron microscope (Jeol Japan 6000), the surface morphology and shape of the best formulation of silver nanoparticles obtained from the produced batches were examined. The batches that showed an appropriate balance between the percentages released were the focus of the examination. A high vacuum evaporator was used to finely sputter the sample after it had been adhered on carbon tape. 10 kV was used as the acceleration voltage during the scanning procedure. A range of magnifications were used to take microphotographs, with a higher magnification of 200X being used especially to study the surface morphology (Prakash et al., 2013).

Formulation of silver nanoparticles incorporated hydrogel

The preparation of various silver nanoparticle-incorporated hydrogel formulations involved dissolving a calculated amount of polyacrylic acid polymer (carbopol 934), chitosan, and honey hydrogel while continuously stirring with a magnetic stirrer for one hour until the polymer was soaked in water. To keep the pH of the carbopol hydrogel stable, TEA was added while being constantly stirred. After adding the required quantity of methyl paraben as a preservative, the polymer was allowed to fully expand and equilibrate for 24 hours. Lastly, silver nanoparticles were added to the prior mixture while being continuously stirred until the honey and silver nanoparticles were completely distributed throughout the hydrogel. The aqueous solution was used to reach the final weight of 100g. To finish the hydrogel formation, the finished formulations were put in wide mouth glass containers with screw plastic lids and refrigerated (El-Kased et al., 2017).

Table 2: Different composition of different silver nanoparticles incorporated hydrogel

Composition	G1	G2	G3	G4	G5	G6
Silver nanoparticles eq to (%)	1	1	1	1	1	1
Carbopol 934 (%)	1.0	1.5	2.0	2.5	3.0	3.5
Chitosan (%)	0.5	1.0	1.5	0.5	1.0	1.5
Honey (%)	-	-	-	0.25	0.5	1.0
Triethanolamine (%)	0.2	0.2	0.2	0.2	0.2	0.2
Methyl paraben (%)	0.02	0.02	0.02	0.02	0.02	0.02
Distilled water (ml)	100	100	100	100	100	100

CHARACTERIZATION OF HYDROGEL

pH measurements

A digital pH meter was used to measure the pH of a few chosen optimised formulations (Guptal et al., 2010). A buffer solution of pH 4, pH 7, and pH 9.2 should be used to calibrate the pH meter prior to each pH measurement. The electrode was dipped into the vesicles as long as they were covered after calibration. After that, the pH of the chosen formulation was measured, and the displayed readings were recorded (Sun et al., 2007).

Measurement of viscosity

Using spindle number 63 and an ideal speed of 10 rpm, the Brookfield viscometer was used to measure the viscosity of the manufactured topical hydrogel. The viscosity results are displayed in the table (Kiyotake et al., 2019).

Drug content

The drug content of topical hydrogel is displayed in the table (Afshar et al., 2020). A precisely weighed quantity of gel formulation equal to 20 mg of topical hydrogel gel was taken in a beaker and added 20 ml of methanol. The mixture was then thoroughly mixed and filtered using a 0.45µ membrane filter. A volumetric flask with a capacity of 10 mL was then filled with 0.1 mL of the filtered solution up to 10 mL of methanol. Take 2ml of this solution and react with 1ml of 2% $AlCl_3$ and take the absorbance at 420nm.

Extrudability study

The amount of gel that extruded from the collapsable tube when a specific load was applied was the basis for extrudability. Better extrudability is demonstrated by a larger amount of gel extruded. The weight was applied to a collapsable tube filled with gel, and the weight on which the gel was extruded from the tube was noted (Kesharwani et al., 2022). The table displays the gel's extrudability results.

Spreadability

The formulation must be spreadable in order to offer enough dose for the skin to absorb and have a positive therapeutic effect. A device that has a slide that is fastened to a wooden block and an upper slide that is moveable, with one end of the movable slide secured with a weight pan. In order to assess spreadibility, 2–5 g of gel were placed between two slides, and weight was progressively raised by adding it to the weight pan. The amount of time it took for the top plate to cover 6 cm after adding 20 g of weight was recorded. According to Rughinis et al. (2024), a high spreadability indicates a shorter time to spread.

$$Spreadibility\,(g.cm/\sec) = \frac{Weight\ tide\ to\ Upper\ Slide \times Lenth\ moved\ on\ the\ glass\ slide}{Time\ taken\ to\ slide}$$

In-vitro drug diffusion study

The Franz Diffusion Cell is used to conduct the in-vitro diffusion studies. The membrane of an egg is considered semi-permeable for diffusion. The receptor compartment of the Franz diffusion cell has an effective surface area of permeation of 3.14 square centimetres and an effective volume of about 60 millilitres (Gonullu et al., 2015). The donor and receptor compartments are separated by the egg membrane. A two-centimeter patch that has been weighed and measured is put on the donor compartment's membrane-facing side. Phosphate buffer pH 7.4 serves as the receptor media. To keep the temperature at 32 ± 0.5°C, a water jacket is placed around the receptor chamber. A magnetic stirrer and a thermostatic hot plate are used to

provide heat. The receptor fluid is stirred by Teflon coated magnetic bead which is placed in the diffusion cell.

During each sampling interval, samples are withdrawn and replaced by equal volumes of fresh receptor fluid on each sampling. The samples withdrawn are analyzed spectrophotometrically (Rughinis et al., 2024).

In-vitro anti microbial activity optimized Silver nanoparticles of Celastrus orbiculatus

The well diffusion method was used to evaluate the antibacterial activity of gel and ethanolic extract prepared from Celastrus orbiculatus in accordance with standard procedure (Bharathi et al., 2013). In the studies, three concentrations of extracted and silver nanoparticles 7.5, 15, and 30 mg/ml were utilized. Its key component is the placement of antibiotic-containing wells on the agar surfaces as soon as the organism being tested is inoculated. It is never advisable to utilize undiluted overnight broth cultures as inoculums. After 24 hours of incubation at 37°C, the plates were checked for distinct zones of inhibition surrounding the wells that had been impregnated with a specific drug concentration.

RESULTS AND DISCUSSION

The formulation and evaluation of silver nanoparticles (AgNPs) synthesized using plant extract, followed by hydrogel formulation development were successfully carried out. The percentage yield, entrapment efficiency, and particle size of all nanoparticle formulations (F1–F9) are summarized in Table 1. Among them, formulation F2 showed the most promising characteristics, with the highest entrapment efficiency (82.25 ± 0.32%), a high percentage yield (83.32 ± 2.35%), and the smallest particle size (89.98 nm), making it the optimized formulation for further study.

The FTIR spectra of both the extract and optimized AgNPs (Figures 1 and 2) confirmed the presence of characteristic functional groups such as hydroxyl and carbonyl, which likely played a role in the reduction and stabilization of nanoparticles. UV–Vis spectroscopy (Figure 3) further validated the successful formation of AgNPs by showing characteristic absorption peaks, while SEM imaging (Figure 4) revealed the morphology and confirmed nanoscale particle size for the F2 formulation.

The hydrogel formulations G1 to G6 were evaluated for drug content, viscosity, pH, spreadability, and extrudability (Table 2). Formulation G3 demonstrated the highest drug content (4.05 ± 0.25 mg/100 mg), ideal viscosity (6645 ± 15 cps), acceptable pH (6.80 ± 0.15), good spreadability (9.85 ± 0.15 gm.cm/sec), and adequate extrudability (168 ± 12 g), making it the optimal gel formulation.

The in-vitro drug release profile of G3 (Table 3) showed a sustained release pattern, reaching 93.32% drug release at 300 minutes. The data fitted best with the Higuchi model (r^2 = 0.9779), indicating a diffusion-controlled release mechanism, followed closely by the Korsmeyer-Peppas model (r^2 = 0.9704), suggesting non-Fickian transport (Table 4).

The antimicrobial activity results highlight the superior efficacy of silver nanoparticle gel (G3) compared to the ethanolic extract. While the ethanolic extract exhibited modest inhibition zones against Staphylococcus aureus and Klebsiella pneumoniae (up to 11 mm, Table 5), the G3 gel demonstrated significantly larger zones of inhibition (up to 27 mm, Table 6). This enhancement is likely due to the improved bioavailability and antimicrobial action of silver nanoparticles. The study validates that biosynthesized AgNPs incorporated into a hydrogel system not only enhance drug release and skin applicability but also significantly boost antimicrobial effectiveness compared to the crude plant extract. These findings support the potential of green synthesized AgNP hydrogels as effective topical antimicrobial agents.

Table 3: Results of Percentage yield, Entrapment efficiency (%) and Particle Size

S. No.	F. Code	Percentage yield	Entrapment efficiency (%)	Particle Size

				(nm)
1	F1	80.36±1.25	76.65±0.25	110.25
2	F2	83.32±2.35	82.25±0.32	89.98
3	F3	78.85±1.85	75.65±0.45	105.65
4	F4	73.32±1.65	72.25±0.36	120.25
5	F5	75.65±1.32	73.15±0.22	125.65
6	F6	70.12±2.85	68.88±0.18	115.65
7	F7	69.98±3.65	65.58±0.33	128.98
8	F8	68.85±2.74	63.12±0.45	132.65
9	F9	69.58±2.65	65.74±0.32	136.41

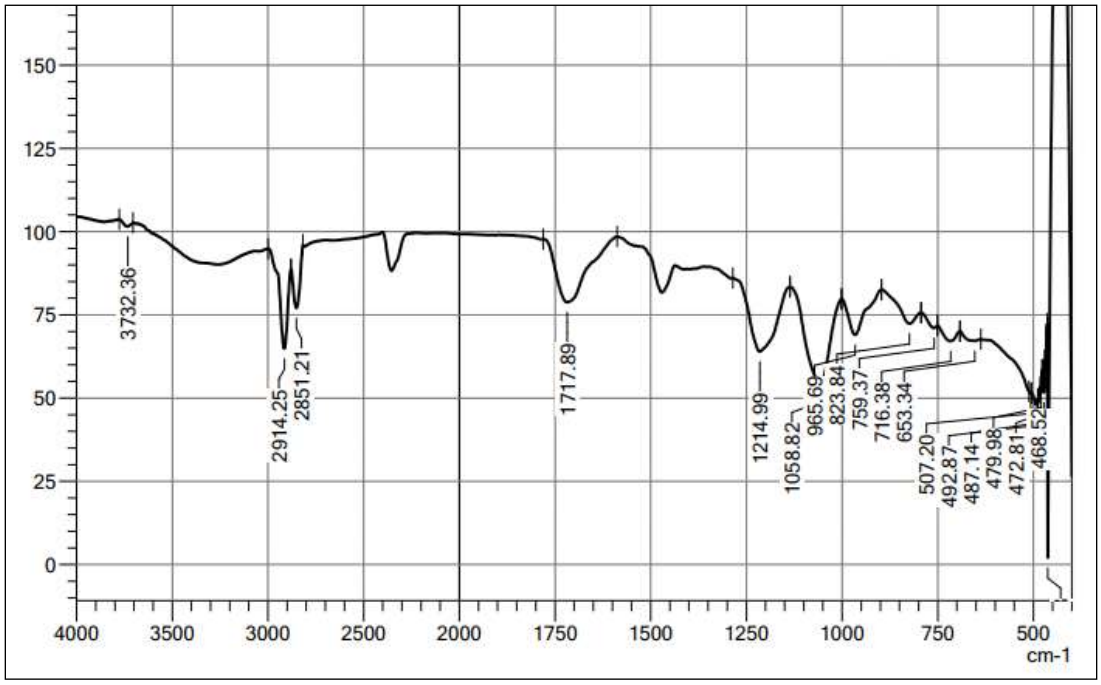

Figure 1: Graph of FT-IR of Extract

International Journal of Environmental Sciences
ISSN: 2229-7359
Vol. 11 No. 7s, 2025
https://www.theaspd.com/ijes.php

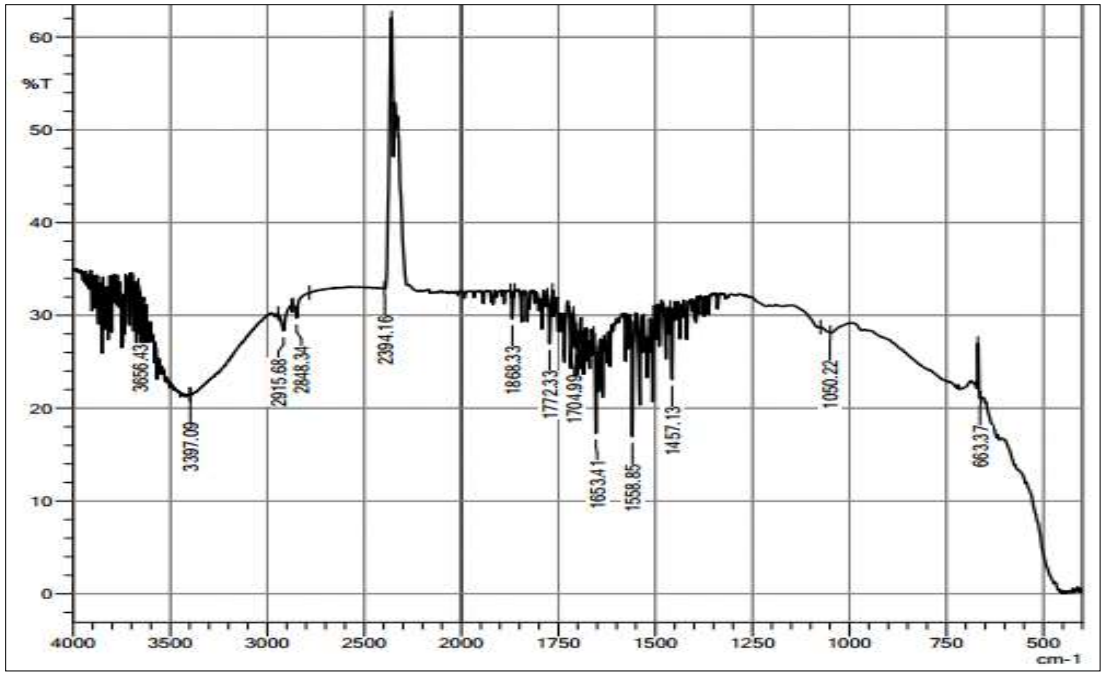

Figure 2: Graph of FT-IR of optimized formulation of silver nanoparticles F2

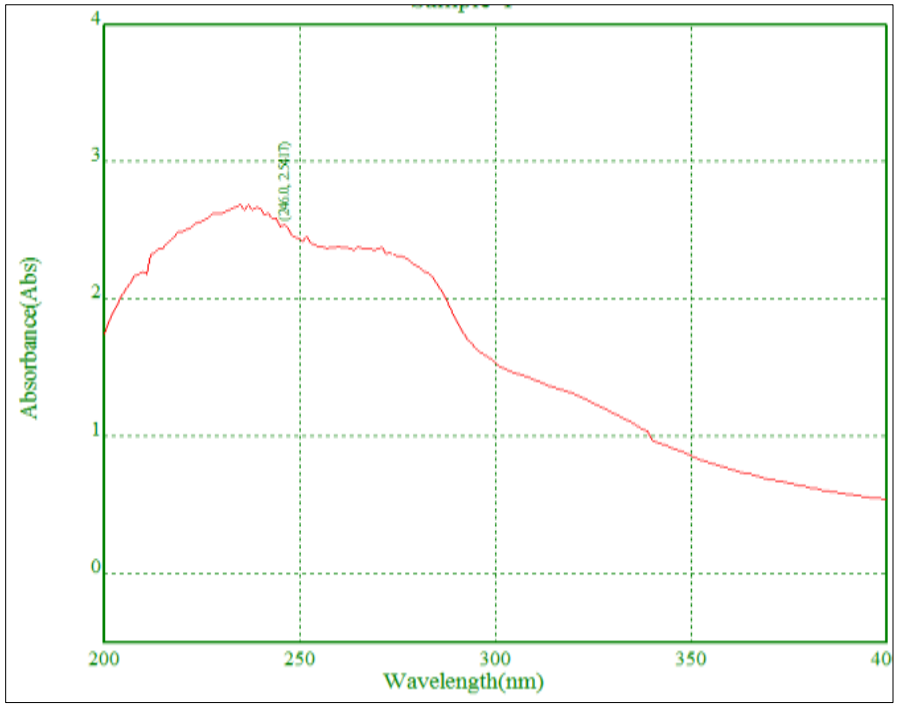

(a)

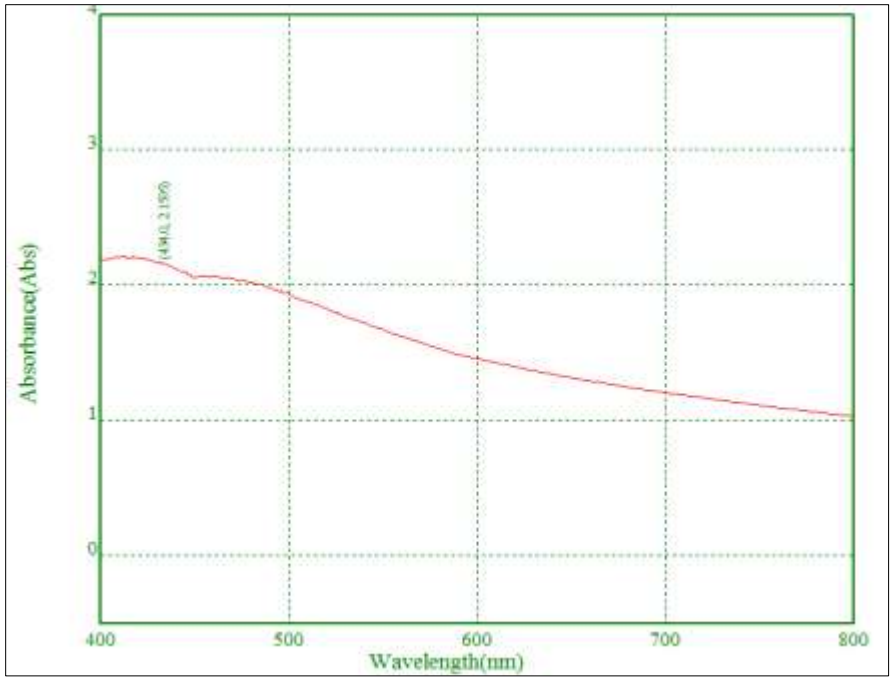

(b)

Figure 3: Graph of UV Vis. Spectroscopy of optimized formulation of extract (a) and optimized formulation of silver nanoparticles F2 (b)

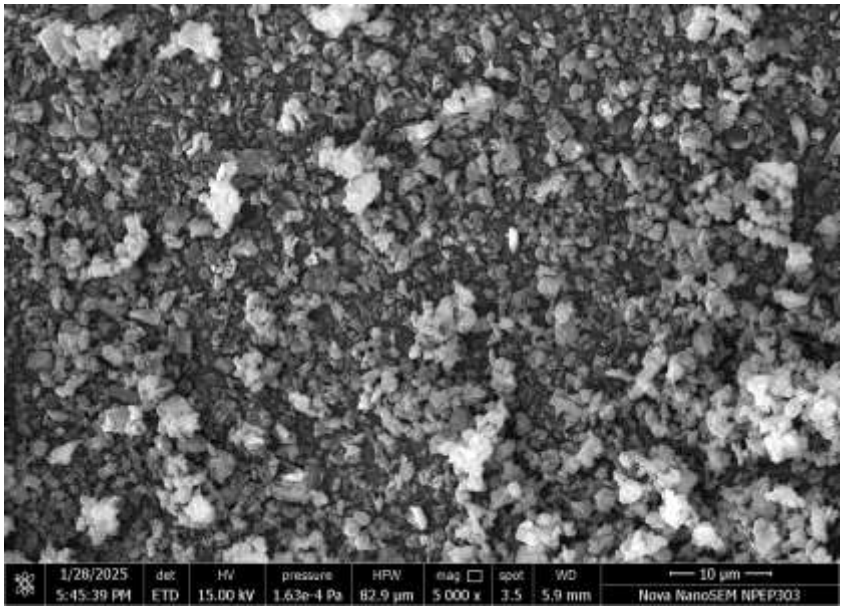

Figure 4: Image of scanning electron microscopy (SEM) of optimized formulation F2

Table 4: Results of evaluation of hydrogel formulations G1 to G6

S. No.	F. Code	% Drug Content	Viscosity (Cps)	pH	Spreadability (Gm.cm/sec.)	Extrudability (g)

		(Total flavonoids content, mg/100mg)				
1	**G1**	2.85±0.85	6825±12	6.92±0.05	11.85±0.35	182±13
2	**G2**	3.22±0.32	6732±10	6.95±0.09	10.23±0.25	175±15
3	**G3**	4.05±0.25	6645±15	6.80±0.15	9.85±0.15	168±12
4	**G4**	3.85±0.41	6645±13	6.78±0.13	12.45±0.33	170±10
5	**G5**	3.47±0.33	6542±10	6.65±0.12	11.32±0.65	163±16
6	**G6**	3.65±0.25	6325±11	6.72±0.18	10.58±0.14	155±14

*Average of three readings

Table 5: In-vitro drug release data for G3

Time (h)	Square Root of Time(h)$^{1/2}$	Log Time	Cumulative* % Drug Release	Log Cumulative % Drug Release	Cumulative % Drug Remaining	Log Cumulative % Drug Remaining
15	3.873	1.176	9.85	0.993	90.15	1.955
30	5.477	1.477	18.96	1.278	81.04	1.909
60	7.746	1.778	38.85	1.589	61.15	1.786
120	10.954	2.079	59.98	1.778	40.02	1.602
180	13.416	2.255	69.98	1.845	30.02	1.477
240	15.492	2.380	73.32	1.865	26.68	1.426
300	17.321	2.477	93.32	1.970	6.68	0.825

*Average of three readings

Table 6: Regression analysis data for optimized formulation G3

F. Code	Zero order	First order	Higuchi	Korsmeyer Peppas
G3	0.9274	0.9044	0.9779	0.9704

Table 7: Antimicrobial activity of ethanolic extract against selected microbes

S. No.	Microbes	Zone of Inhibition (mm)		
		7.5mg/ml	15 mg/ml	30mg/ml
1.	Staphylococcus aureus	7±0.5	9±0.86	10±0
2.	Klebsiella pneumoniae	7±0.3	9±0.57	11±0.5

Table 8: Antimicrobial activity of silver nanoparticles gel (G3) against selected microbes

S. No.	Name of microbes	Zone of inhibition (mm)		
		7.5mg/ml	15 mg/ml	30mg/ml

1.	Staphylococcus aureus	21±0	24±0.47	25±0.57
2.	Klebsiella pneumoniae	24±0	25±0	27±0.5

CONCLUSION

The present study successfully demonstrated the green synthesis of silver nanoparticles (AgNPs) using the ethanolic extract of Celastrus orbiculatus and their incorporation into hydrogel formulations. Among the formulations, F2 was identified as the optimized nanoparticle formulation based on its high entrapment efficiency, desirable particle size, and percentage yield. The optimized hydrogel formulation G3 exhibited excellent physicochemical properties, including high drug content, suitable viscosity, spreadability, pH, and extrudability. The in-vitro drug release profile of G3 followed a sustained release pattern best explained by the Higuchi model, indicating diffusion-controlled drug release. Furthermore, the AgNP-loaded hydrogel showed significantly enhanced antimicrobial activity against Staphylococcus aureus and Klebsiella pneumoniae compared to the crude extract, confirming the synergistic effect of silver nanoparticles and phytochemicals. the findings support the potential of Celastrus orbiculatus-based silver nanoparticle hydrogel as an effective and natural topical antimicrobial agent, paving the way for further preclinical and clinical evaluations in wound healing and dermatological applications.

REFERENCES

1. Rai, M., Yadav, A., & Gade, A. (2009). Silver nanoparticles as a new generation of antimicrobials. Biotechnology Advances, 27(1), 76–83. https://doi.org/10.1016/j.biotechadv.2008.09.002
2. Iravani, S., Korbekandi, H., Mirmohammadi, S. V., & Zolfaghari, B. (2014). Synthesis of silver nanoparticles: chemical, physical and biological methods. Research in Pharmaceutical Sciences, 9(6), 385–406.
3. Xiao, X., Xu, W., Zhang, Y., & Sun, J. (2015). Antioxidant and antibacterial properties of Celastrus orbiculatus extract. Pharmaceutical Biology, 53(5), 761–767. https://doi.org/10.3109/13880209.2014.936463
4. Kora, A. J., & Arunachalam, J. (2011). Green synthesis of silver nanoparticles using Azadirachta indica gum and their antibacterial activity. International Journal of Nanomedicine, 6, 1–8. https://doi.org/10.2147/IJN.S16297.
5. Raghunandan, D., Mahesh, B.D., Basavaraja, S. et al. (2011). Journal of Nano Research, 13, 2021–2028.
6. Bahuguna G, et al. Green synthesis and characterization of silver nanoparticles using aqueous petal extract of the medicinal plant Combretum indicum. Mat Res Express. 2016; 3(7):075003.
7. Bar H, et al. Green synthesis of silver nanoparticles using seed extract of Jatropha curcas. Colloids Surf A Physicochem Eng Asp. 2009; 348(1–3):212–6.
8. Guzman MG, Dille J, Godet S. Synthesis of silver nanoparticles by chemical reduction method and their antibacterial activity. Int J Chem Biomol Eng. 2009;2(3):104–11.
9. Ibrahim HM. Green synthesis and characterization of silver nanoparticles using banana peel extract and their antimicrobial activity against representative microorganisms. J Radiat Res Appl Sci. 2015; 8(3):265–75.
10. Kumar VG, et al. Facile green synthesis of gold nanoparticles using leaf extract of antidiabetic potent Cassia auriculata. Colloids Surf B: Biointerfaces. 2011;87(1):159–63.
11. Prakash P, et al. Green synthesis of silver nanoparticles from leaf extract of Mimusops elengi, Linn. for enhanced antibacterial activity against multi drug resistant clinical isolates. Colloids Surf B: Biointerfaces. 2013; 108:255–9.

12. D. Bharathi, M. Diviya Josebin, S. Vasantharaj, V. Bhuvaneshwari. Biosynthesis of silver nanoparticles using stem bark extracts of Diospyros montana and their antioxidant and antibacterial activities.J. Nanostructure Chem., 8 (2018), pp. 83-92.